

## ARTICLE OPEN



# CREB5 promotes the proliferation and self-renewal ability of glioma stem cells

Hyun-Jin Kim<sup>1,10</sup>, Hye-Min Jeon<sup>2,10</sup>, Don Carlo Batará<sup>1</sup>, Seongsoo Lee<sup>3</sup>, Suk Jun Lee<sup>4</sup>, Jinlong Yin<sup>5</sup>, Sang-Ik Park<sup>6</sup>, Minha Park<sup>7</sup>, Jong Bae Seo<sup>7</sup>, Jinik Hwang<sup>8</sup>, Young Joon Oh<sup>9</sup>, Sung-Suk Suh<sup>7✉</sup> and Sung-Hak Kim<sup>1✉</sup>

© The Author(s) 2024

Glioblastoma multiforme (GBM) is the most fatal form of brain cancer in humans, with a dismal prognosis and a median overall survival rate of less than 15 months upon diagnosis. Glioma stem cells (GSCs), have recently been identified as key contributors in both tumor initiation and therapeutic resistance in GBM. Both public dataset analysis and direct differentiation experiments on GSCs have demonstrated that CREB5 is more highly expressed in undifferentiated GSCs than in differentiated GSCs. Additionally, gene silencing by short hairpin RNA (shRNA) of CREB5 has prevented the proliferation and self-renewal ability of GSCs in vitro and decreased their tumor forming ability in vivo. Meanwhile, RNA-sequencing, luciferase reporter assay, and ChIP assay have all demonstrated the closely association between CREB5 and OLIG2. These findings suggest that targeting CREB5 could be an effective approach to overcoming GSCs.

*Cell Death Discovery* (2024)10:103; <https://doi.org/10.1038/s41420-024-01873-z>

## INTRODUCTION

Glioblastoma multiforme (GBM) is the most common and malignant brain tumor. Despite treatment options such as surgical resection, radiotherapy, and chemotherapy, the median survival rate following diagnosis is only 15 months [1, 2]. There is accumulating evidence that glioma stem cells (GSCs), also known as tumor initiating cells, play an important role in tumor recurrence and resistance to treatments [3, 4]. As such, studies that target the pro-tumorigenic features of GSCs are promising approaches that could lead to long term treatments for GBM.

CREB5, also known as CREB-BPA, belongs to the CREB (cAMP response element-binding protein) protein family, which is known to regulate cell growth, proliferation, and differentiation by binding to the cAMP-response elements through their domain bZIP DNA-binding and zinc-finger domains. Several studies have shown the diverse roles of CREB5, especially its involvement in tumor progression in various cancers [5–7]. For instance, it has been found that increased CREB5 expression is positively correlated with tumor cell invasion and a poor prognosis for cancer patients with epithelial ovarian cancer and hepatocellular carcinoma [8, 9]. Similarly, in colorectal cancer, in depth computational analysis has shown the involvement of CREB5 in the metastatic signal network, suggesting that it promotes metastasis and invasiveness by boosting MET expression and

activating the HGF-MET signaling pathway [10]. On the other hand, in prostate cancer, CREB5 has been found to play a crucial role in promoting resistance to androgen receptor antagonists and androgen deprivation [11].

In this study, we demonstrate the role of CREB5 in glioblastoma, particularly in GSCs. We found that the knockdown of CREB5 in GSCs inhibited its proliferation and self-renewal activity in vitro and tumor forming ability in vivo. Interestingly, we found that OLIG2 is significantly downregulated by suppressing CREB5 expression. We also confirmed that CREB5 is highly expressed in GSCs and associated with poor survival in GBM patients. These findings suggest that overexpression of CREB5 is important in GSC progression.

## RESULTS

### CREB5 mRNA is expressed higher in the undifferentiated GSCs

Previous research has demonstrated that undifferentiated GSCs have stronger tumorigenic potential and self-renewal ability than differentiated GSCs [12]. We compared the expression pattern of genes belonging to the CREB family in undifferentiated and differentiated GSCs using a publicly available dataset (GSE4536). Among the CREB family, CREB5 expression was the highest in undifferentiated GSCs (“NBE” conditions: serum free DMEM/F12

<sup>1</sup>Department of Animal Science, College of Agriculture and Life Sciences, Chonnam National University, Gwangju 61186, Republic of Korea. <sup>2</sup>Department of Cancer Biology, Lerner Research Institute, Cleveland Clinic, Cleveland, OH, USA. <sup>3</sup>Gwangju Center, Korea Basic Science Institute (KBSI), Gwangju 61186, Republic of Korea. <sup>4</sup>Department of Biomedical Laboratory Science, College of Health & Medical Sciences, Cheongju University, Chungbuk 360764, Republic of Korea. <sup>5</sup>Henan-Macquarie Uni Joint Centre for Biomedical Innovation, Academy for Advanced Interdisciplinary Studies, Henan Key Laboratory of Brain Targeted Bio-nanomedicine, School of Life Sciences, Henan University, Kaifeng 475004 Henan, China. <sup>6</sup>Laboratory of Veterinary Pathology, BK21 FOUR Program, College of Veterinary Medicine, Chonnam National University, Gwangju 61186, Republic of Korea. <sup>7</sup>Department of Biomedicine, BK21 FOUR Program, Health & Life Convergence Sciences, Biomedical and Healthcare Research Institute, Mokpo National University, Muan 58554, Republic of Korea. <sup>8</sup>West Sea Fisheries Research Institute, National Institute of Fisheries Science, Incheon 22383, Republic of Korea. <sup>9</sup>Technology Innovation Research Division, World Institute of Kimchi, Gwangju 61755, Republic of Korea. <sup>10</sup>These authors contributed equally: Hyun-Jin Kim, Hye-Min Jeon. ✉email: [sungsuksuh@mokpo.ac.kr](mailto:sungsuksuh@mokpo.ac.kr); [sunghakkim@jnu.ac.kr](mailto:sunghakkim@jnu.ac.kr)

Received: 16 April 2023 Revised: 7 February 2024 Accepted: 15 February 2024

Published online: 28 February 2024

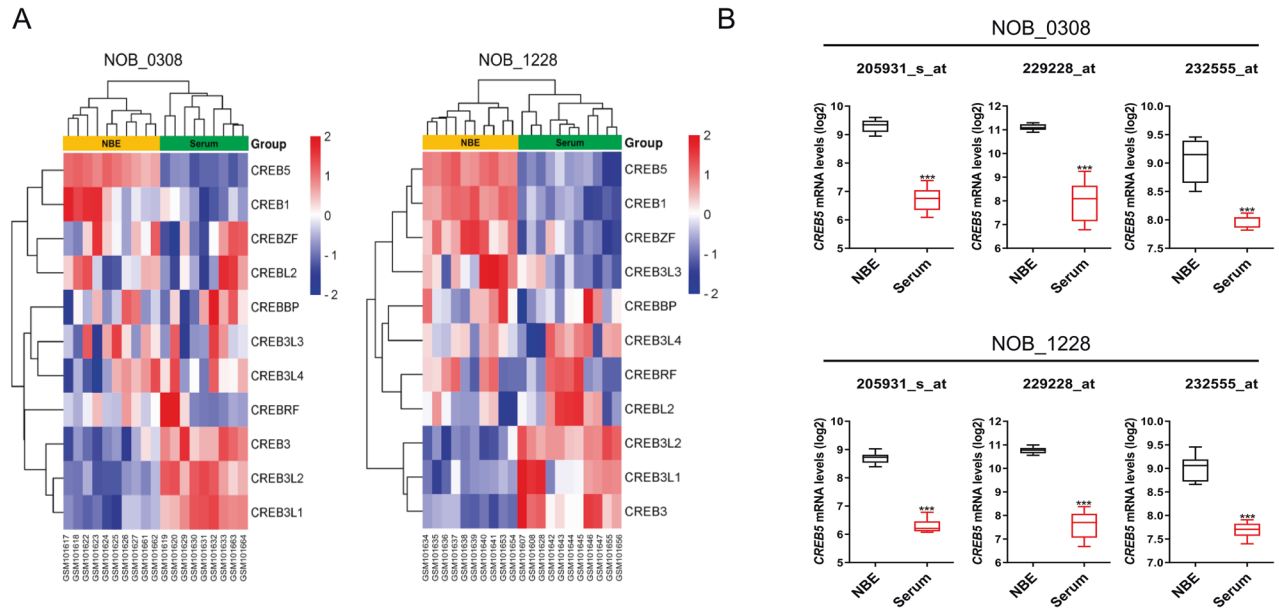


**Fig. 1** CREB5 mRNA is expressed higher in the undifferentiated GSC. **A, B** The comparison of CREB Family expression in GSCs cultured under NBE and Serum conditions according to multiple probes set of the GSE4536 dataset. **A** 0308 cells; **B** 1228 cells. Data are means  $\pm$  SEM (NBE,  $n = 10$  or  $11$ ; FBS,  $n = 11$  or  $10$ ). \*\*\* $p < 0.001$ .

media supplemented with basic FGF and EGF), while lowly expressed in differentiated GSCs ("Serum" conditions: DMEM/F12 media containing 10% FBS) (Fig. 1A, B). These findings suggest that CREB5 may play an essential role in the maintenance of GSCs.

#### CREB5 expression is correlated with poor prognosis

We also investigated the clinical relevance of CREB5 in GBM patients by examining the expression patterns and survival rates of the CREB family using the Rembrandt dataset. We first compared the expression of the CREB family genes in non-tumor and GBM patients. We found that several genes, including CREB5, were highly expressed in GBM (Supplementary Fig. S1A). Next, we analyzed the expression of CREB family genes according to glioma grade and observed that some genes, including CREB5, were highly expressed in grade IV GBM compared to grade II or III (Supplementary Fig. S1B). We also evaluated the survival rates of glioma patients based on the expression levels of CREB family genes. Our investigation revealed that only high expression of CREB5 was significantly associated with poor survival rates in GBM patients (Supplementary Fig. S1C). The link between high CREB5 expression and poor overall survival, as well as the increased expression of CREB5 in GBM, supports CREB5's potential as a promising target in GBM.

#### CREB5 is overexpressed in the classical subtype and highly expressed in the cellular tumor region and pseudopalisading cells around necrosis

GBM subtypes could be classified into proneural, classical, mesenchymal, and neural types based on genome wide analysis of mRNA expression in 300 GBM patient tissues [13]. We found that CREB5 mRNA is highly expressed in the classical subtype in the Rembrandt dataset (Supplementary Fig. S2A). Moreover, in the classical GBM subtype, a correlation was confirmed between the CREB5 gene and genes important for stemness of glioma stem cells, such as OLIG2 and NES (Supplementary Fig. S2B). To identify the GBM anatomical region where CREB5 is preferentially expressed, we compared its expression patterns in the leading edge (LE), infiltrating tumor (IT), cellular tumor (CT), perinecrotic zone (PNZ), pseudopalisading cells around necrosis (PAN), hyperplastic blood vessels in cellular tumors (HBV), and microvascular

proliferation (MVP) using the Ivy Glioblastoma Atlas Project dataset. We found that CREB5 is highly enriched in the CT and PAN regions (Supplementary Fig. S2C).

#### CREB5 is highly expressed in GSCs

To validate the expression patterns of CREB5 in gliomas, we analyze the mRNA expression of CREB5 in glioma cell lines. We found that GSCs had considerably higher levels of CREB5 expression when compared to non-stem cell glioma cells and normal human astrocytes (NHA) (Fig. 2A). Next, we cultured GSCs in FBS containing media for seven days to generate differentiated GSCs. The expression of stem cell markers decreased substantially in differentiated GSCs, while differentiation markers were significantly elevated. Also, differentiated GSCs had lower CREB5 expression than their undifferentiated counterparts (Fig. 2B, C). Based on these results, we suggest that the expression of CREB5 is significantly elevated in GSCs.

#### Suppressing of CREB5 inhibits proliferation and self-renewal ability in GSCs

We next investigated the role of CREB5 in the proliferation and self-renewal ability of GSCs. Upon silencing the expression of CREB5, we observed a decrease in the proliferation of GSC11 and GSC23 cells (Fig. 3A, B). The Annexin V/PI assay also demonstrated that inhibition of CREB5 expression caused a shift in the distribution of GSCs towards apoptotic or necrotic regions (Fig. 3C). On the other hand, we observed that a decrease in CREB5 expression led to the suppression of GSC sphere growth (Fig. 3D). To ascertain the effects of decreased CREB5 expression on the self-renewal activity of GSCs, we carried out the serial limiting dilution assay. We confirmed a significant reduction in the characteristic of stem cell in GSCs when CREB5 expression was inhibited (Fig. 3E). These findings indicate that inhibition of CREB5 expression leads to decreased proliferation and self-renewal ability of GSCs.

#### The inhibition of CREB5 reduces the tumorigenic potential of GSCs in vivo

Using an in vivo orthotopic xenograft model, we evaluated the tumorigenic potential of CREB5. After suppressing the expression of CREB5 using shCREB5 in GSC11 cells, we noticed a significant

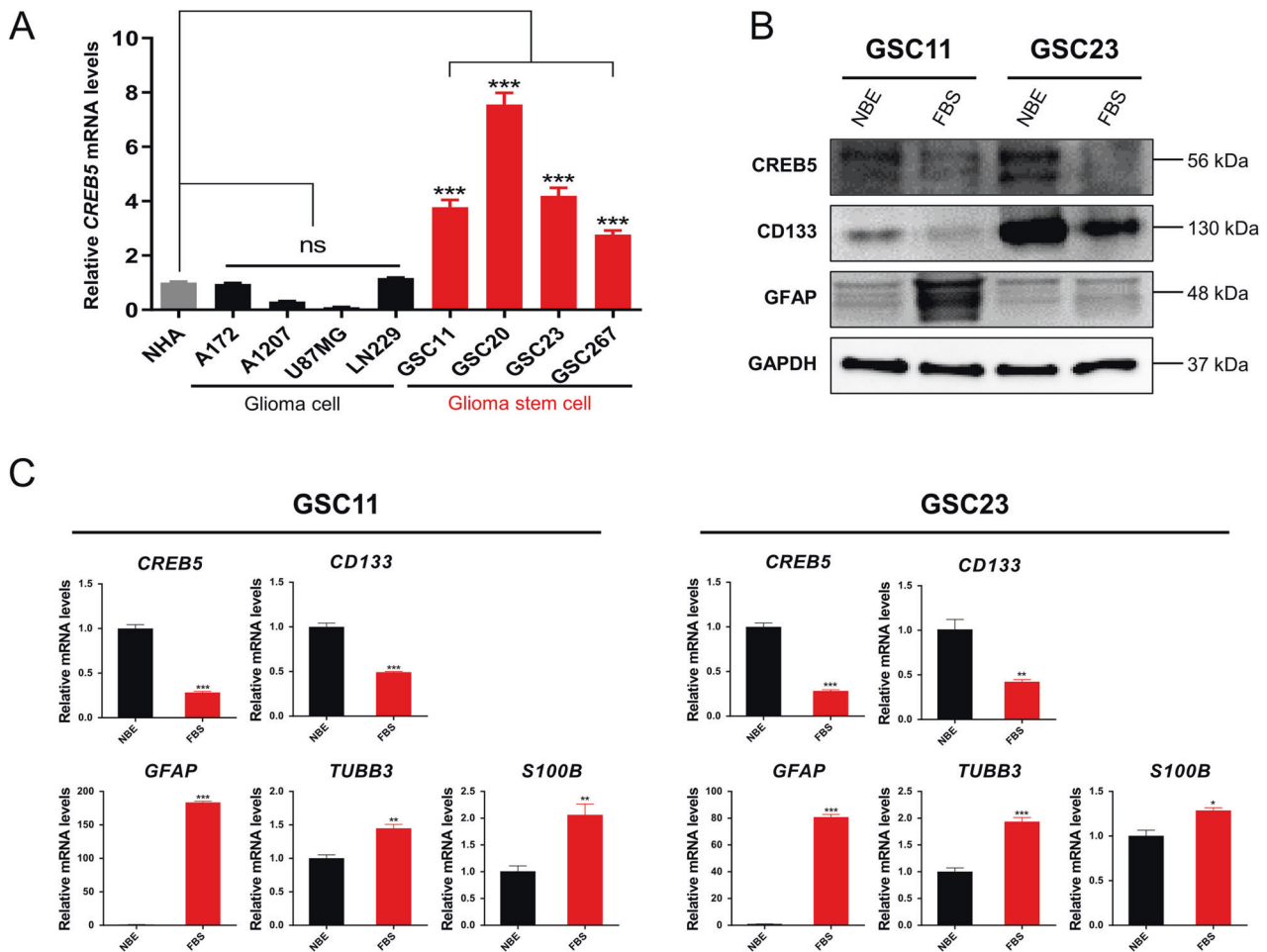


**Fig. 2** CREB5 is expressed highly expressed in GSC. **A** RT-qPCR analysis of CREB5 mRNA expression in NHA, non-stem cell glioma cells, and GSCs. **B** Western blot analysis of CREB5 protein in GSCs and differentiated GSCs. **C** RT-qPCR analysis of mRNA expressions in GSCs and differentiated GSCs. Data are means  $\pm$  SEM ( $n = 3$ ). \* $p < 0.05$ , \*\* $p < 0.01$ , \*\*\* $p < 0.001$ .

decrease in the tumorigenic potential of knockdown cells compared to shNT(Non-target) control after injection into the brains of nude mice (Fig. 4A, B). We also observed there is a significant increase in mouse survival when inoculated with CREB5 knockdown GSCs (Fig. 4C). These data suggest that CREB5 could play an important role in the tumorigenic potential of GSCs in vivo.

#### RNA-Sequencing reveals pathways and genes downregulated by shCREB5

To understand the mechanism of how CREB5 regulates GSCs at the transcriptional level, we performed an RNA-sequencing analysis (Fig. 5A). KEGG pathway and Gene Ontology Biological Process analysis on the RNA-sequencing data revealed that upon CREB5 knockdown, the expression of genes that are related to multiple cancer stem cell associated signaling pathways, and cell cycle pathway were also decreased (Fig. 5B). These findings suggest the importance of CREB5 expression in the regulation of pathways that are important in GSC progression.

#### CREB5 binds to the AP-1 sites within the OLIG2 promoter

Next, we identified downstream genes that are concomitantly decreased upon CREB5 inhibition in GSCs. The genes such as OLIG2, DUSP5, NFIX, ZCCHC24, VIM, and SPARCL1 were concurrently downregulated in both GSC11 and GSC23 cells (Fig. 6A). OLIG2 is a gene involved in central nervous system development, and there are reports that this gene plays an important role in the

maintenance of brain tumors, especially GSCs [14–16]. Accordingly, OLIG2 is highly expressed in GSCs and that cell proliferation is suppressed when it is inhibited [17]. Therefore, taking into account the fact that CREB5 is a transcription factor and the downregulation of OLIG2 at the transcriptional level, we investigated whether CREB5 influences the activity of the OLIG2 promoter using a luciferase reporter assay (Fig. 6B). As a result, we observed an increase in OLIG2 promoter activity upon over-expression of CREB5 in HEK293T cells in a concentration dependent manner (Fig. 6B). Furthermore, we performed chromatin immunoprecipitation (ChIP) assay and identified multiple AP-1 sites within the OLIG2 promoter where CREB5 protein could potentially bind (Fig. 6C) [10]. Consistently, we found a positive correlation between CREB5 and OLIG2 expression in GBM by utilizing various patient datasets (Supplementary Fig. S3). These findings confirm that OLIG2 is a transcriptional target of CREB5.

#### DISCUSSION

Among CREB family proteins, CREB5 is specifically highly expressed and strongly associated with poor patient survival in GBM. Due to its differential abundance in the GSC population, we investigated the function of CREB5 by suppressing its expression and examining the mechanism to regulate GSC. Interestingly, CREB5 knockdown significantly inhibits GSCs' survival, self-renewal activity in vitro, and tumorigenic potential in a mouse xenograft model. RNA sequencing analysis revealed CREB5 modulates a

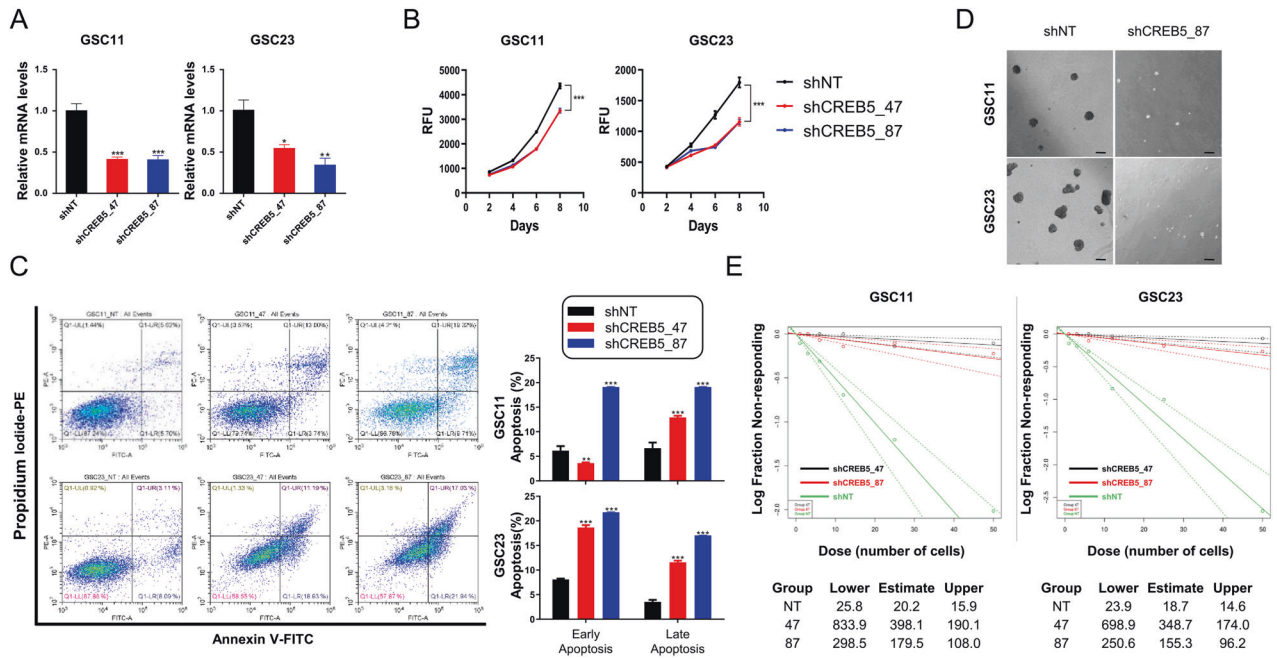


**Fig. 3 Suppressing of CREB5 inhibits proliferation and self-renewal ability in GSCs.** **A** RT-qPCR analysis showing CREB5 knockdown after transduction with shRNA in GSCs. **B** Cell proliferation shCREB5 treated GSCs. **C** Annexin-V/propidium iodide staining of GSCs after transduction with shCREB5. **D** Representative images showing cell spheres. Scale bars = 100  $\mu$ m. **E** An in vitro limiting dilution assay using gradually decreasing cell seeding density shows the cell sphere forming ability of GSCs transduced with shCREB5. Data are means  $\pm$  SEM ( $n = 3$ ). \* $p < 0.05$ , \*\* $p < 0.01$ , \*\*\* $p < 0.001$ .

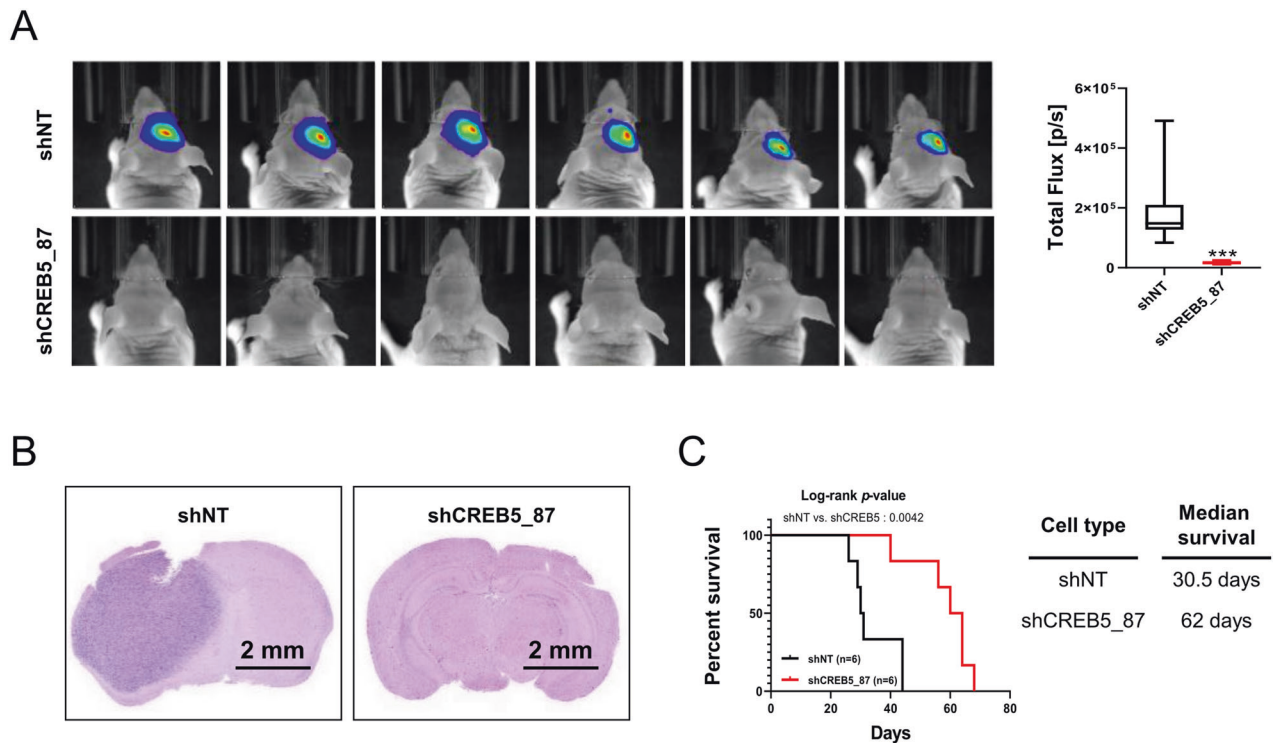


**Fig. 4 The inhibition of CREB5 reduces the tumorigenic potential of GSCs in vivo.** **A** In vivo bioluminescent imaging was performed on nude mice bearing intracranial xenografts derived from shNT (Non-target) and shCREB5 transduced GSC11. Data are means  $\pm$  SEM ( $n = 6$ ). \*\*\* $p < 0.001$ . **B** Representative images of H&E stained coronal sections of tumor bearing brains harvested after implantation of shNT and shCREB5 treated GSC11. Scale bars represent 2 mm. **C** Kaplan-Meier survival curves of nude mice bearing intracranial tumors derived from shNT and shCREB5 treated GSC11.

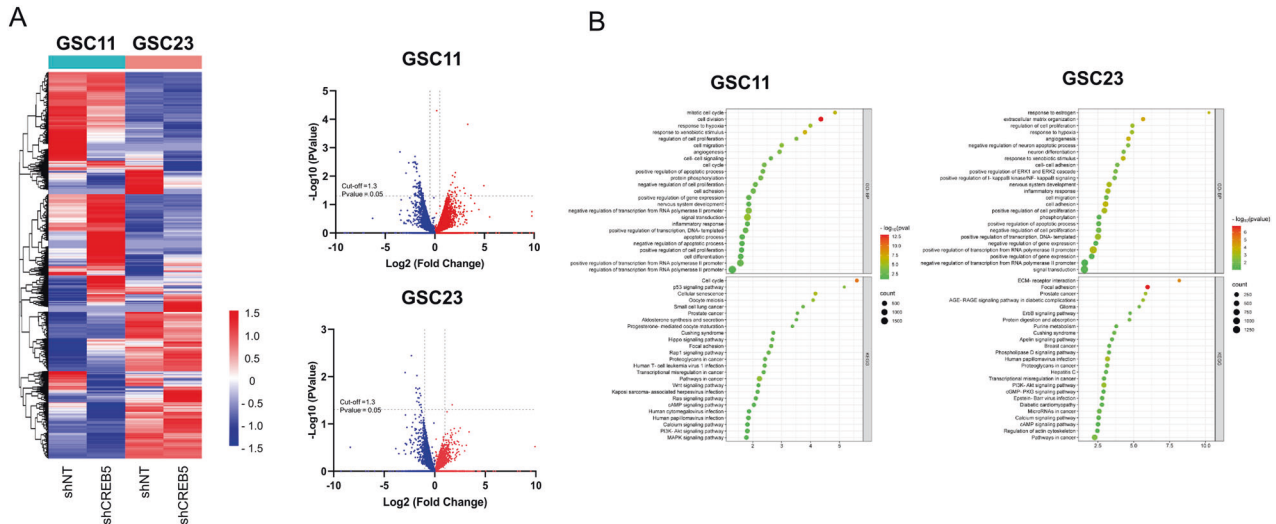


**Fig. 5** RNA-Sequencing reveals pathways and genes downregulated by shCREB5. **A** Heat map and volcano plots of transcriptional regulation patterns of shNT and shCREB5 transduced GSCs. **B** Dot plots present enrichment pathways of genes downregulated with CREB5 in shCREB5 transduced GSCs. Data are means  $\pm$  SEM.

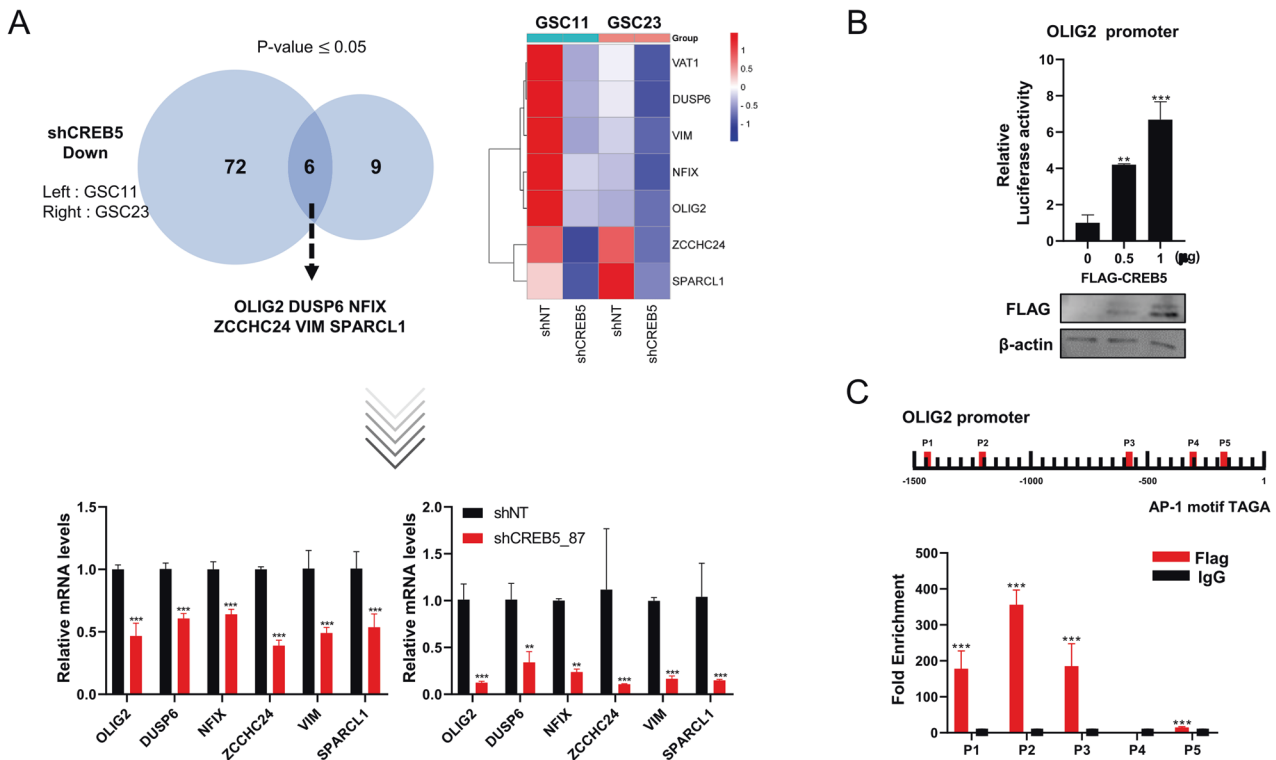


**Fig. 6** CREB5 binds to the AP-1 sites within the OLIG2 promoter. **A** RT-qPCR validation of downregulated genes after CREB5 inhibition. **B** Luciferase assay using OLIG2 promoter after indicated treatment. **C** ChIP analysis of CREB5 binding to the OLIG2 promoter in HEK293T. Data are means  $\pm$  SEM ( $n = 3$ ). \* $p < 0.05$ , \*\* $p < 0.01$ , \*\*\* $p < 0.001$ .

variety of signaling pathways including cell cycle, PI3K-Akt, and focal adhesion. Among the putative target genes of CREB5, we have focused on OLIG2 due to its clinical relevance in GBM.

We then hypothesize the role CREB5-OLIG2 axis in GSCs as follows: 1) as a central nervous system (CNS) restricted transcription factor, it plays an essential role in glial progenitor proliferation [18–20]; (2) it is widely expressed in gliomas and plays a critical role in gliomagenesis and tumor phenotype plasticity; and [15–17, 21–23] (3) recently, OLIG2 has been identified as a core transcription factor, along with SOX2, SALL2, and POU3F2, that

reprograms differentiated GBM cells into GSCs [14]. Therefore, we postulate that CREB5 might regulate OLIG2 to be involved in the maintenance of GSCs.

Meanwhile, we found that CREB5 expression is strongly associated with poor patient survival and upregulated in GBM classical subtype in publicly available datasets. The classical GBM subtype is characterized by a high frequency of EGFR gene amplification and mutation [13]. Aberrant EGFR amplification or mutation may influence the activation of signaling networks that promotes irregular cell growth and survival, ultimately driving

tumor progression [24–26]. EGFR signaling pathways interact with downstream effectors, such as the RAS/RAF/MEK/ERK and PI3K/Akt/mTOR pathways [27, 28] vital for cell communication and interaction, regulating basic cell processes like growth, survival, and differentiation. Interestingly, after inhibiting CREB5 expression, we found that the genes associated with PI3K-Akt signaling were decreased in both GSC11 and GSC23 cells. This suggests that there might be a negative feedback loop that starts from CREB5, suppressing the PI3K-Akt signaling pathway.

On the other hand, RNA-seq data showed that four other genes (DUSP6, NFIX, VIM, and SPARCL1) associated with cancer were also downregulated in CREB5 knockdown cells. The DUSP6 (dual specificity phosphatase 6) is highly expressed in GBM and its expression is associated with poor patient survival [29]. Findings also show that exogenous overexpression of DUSP6 increases tumor growth as well as resistance to cisplatin mediated cell death in both in vitro and in vivo experiments [30]. Interestingly, DUSP6 was identified as hub genes and anti-cancer compounds can be developed by inhibiting the interaction of ERK2 and DUSP6 [29]. Similarly, the NFIX (nuclear factor IX) was also found to be upregulated in GBM and transcriptionally upregulates Ezrin, a protein that crosslinks the cytoskeleton and plasma membrane. Suppression of NFIX in GBM cells impairs cell proliferation and migration in vitro and increases the survival rate in mouse orthotopic xenograft models [31]. It was found that NFIX binds to the promoter of the Go-Ichi-Ni-San 1 (GINS1) gene, regulating GBM cell proliferation. NFIX inhibition in a GINS1 dependent manner, increases the sensitivity of GBM cells to DNA damage inducing agents, such as doxorubicin and temozolomide [32]. VIM (Vimentin) is highly expressed in gliomas compared to non-tumor tissues. Reports show that VIM inhibition reduces the migration ability in GBM cells (U87MG, U251, and U373) [33]. The antivimentin nanobody (Nb79) considerably diminishes the invasion capacity of both the differentiated GBM cell line (U87MG) and the GSC line (NCH421k). Recently, the invasion inhibitory effect of Nb79 was also observed on U87MG and NCH421k in vitro and in vivo in zebrafish embryos [34]. Lastly, proteomics analysis revealed that SPRL1 (Sparc like protein 1), the protein encoded by secreted, acidic, and rich in cysteine like 1 (SPARCL1), is highly expressed in mouse brain tumor xenograft models. Also, the elevated SPRL1 expression is associated with high grade glioma samples [35]. Findings show that overexpression of SPARCL1 promotes neo-angiogenesis in intracranial xenografts derived from proneural and mesenchymal GSCs and endow the angio-architectural pattern in patients. Furthermore, SPARCL1 triggers a notable rise in activated microglia, which corresponds with the augmentation of angiogenesis [36]. As such, additional studies on these other genes and their association with CREB5 expression are important and could provide insights, especially on their role in GBM progression. Meanwhile, in recent studies it was reported that high glucose can activate the PI3K/Akt/CREB5 signaling pathway, resulting in excessive proliferation and migration of vascular smooth muscle cells [37]. Identifying the upstream regulatory elements that affect CREB5 expression and activity in GBM is also necessary.

In conclusion, our data suggest that CREB5 plays a critical role in maintaining GSCs by regulating OLIG2. Targeting CREB5 may be a promising approach not just eradicating GSCs but also improving GBM treatment.

## MATERIALS AND METHODS

### Cell culture

Normal human astrocytes (NHA) were cultured in an astrocyte medium (ScienCell Research Laboratories, USA) supplemented with 10% fetal bovine serum (FBS; Gibco, USA), 1% astrocyte growth supplement (AGS; ScienCell Research Laboratories, USA), and 1% penicillin/streptomycin (P/S; Welgene, Republic of Korea). The glioma cell lines (A172, A1207, U87MG,

LN229) and HEK293T were cultured in Dulbecco's modified medium (DMEM/F12; Welgene, Republic of Korea) supplemented with 10% FBS, and 1% P/S. The glioma stem cells (GSC11, GSC20, GSC23, GSC267) obtained from the University of Texas MD Anderson Cancer Center [38] were cultured in a Neurobasal Medium (NBE) comprising of DMEM/F12, 1% P/S, 2% B27 (Gibco, Thermo Fisher Scientific, USA), epidermal growth factor (EGF; 20 ng/ml; R&D Systems, USA), and basic fibroblast growth factor (bFGF; 20 ng/ml; R&D Systems, USA). All GSC cell lines have been authenticated and are Mycoplasma-free. (COSMO GENETECH, Republic of Korea). All cells were maintained at 37 °C with 5% CO<sub>2</sub>.

### Quantitative reverse transcription-PCR (RT- qPCR)

Total RNA was extracted using RiboEX reagent (GeneAll, Republic of Korea) and purified with the HybridR kit (GeneAll, Republic of Korea) according to the manufacturer's instructions. The RevertAid First Strand cDNA Synthesis Kit (Thermo Fisher Scientific, MA, USA) was used to synthesize cDNA from 500 ng of total RNA. Quantitative Real Time PCR (qPCR) was performed using the TB Green Premix Ex Taq (Tli RNaseH Plus; Takara Korea Biomedical Inc., Korea) on a BioRad Laboratories CFX96 realtime polymerase chain reaction detection system (CA, USA). The cycle threshold (Ct) values from qPCR results were analyzed using the  $2^{-\Delta\Delta C_t}$  method. The following primer sequences (5' to 3') were used for qPCR: 18S (loading control): forward F, CAGCCACCCGAGATTGAGCA and reverse R, TAGTAGCGACGGGCGGTGTG; CREB5: F, GAGCGACAATGTGTCAGTGAACCTC and R, TGAGTCAATGCAGCTTCAACC; CD133: F, CAGGTAAGAACCCTGGATCAA and R, TCAGATCTGTGAACGCCTTG; GFAP: F, GGAACATCTGTTGTAAGACC and R, AGAGCGGAGCAACTATCCT; TUBB3: F, AGTGTGAAAACCTGCGACTGC and R, ACGACGCTGAAGGTGTTCAT; S100B: F, TCAAAGAGCAGGAGTGTG and R, CTGTGGCAGGAGTGAATAC; OLIG2: F, ATGCACGACCTCAACATCGCCA and R, ACCAGTCGCTTCATCTCCTCCA; DUSP6: F, CTCGGATCACTGGAGCCAAAAC and R, GTCACAGTGA CTGAGCGGCTAA; NFIX: F, CGATGACAGTGAGATGGAGAGC and R, GCAGAA GTCCAGCTTCTCTGAC; ZCCHC24: F, CAGGAGTGCATCAAGTGCCACA and R, AGGACCTTGCACTTCTCGAGA; VIM: F, AGGCAAAGCAGGAGTCCACTGA and R, ATCTGGCGTTCAGGACTCAT; SPARCL1: F, GTGAAGCAACATGAGGG TGCA and R, GTTGAGGACAAGTCACTGGATC.

### Western blot analysis

The cells were lysed using a combination of RIPA buffer (Thermo Scientific, CA, USA) and phosphatase inhibitor cocktail 2 obtained from APExBIO Technology LLC (Houston, Texas, USA). To determine the protein content of the lysate, we used the BCA Protein Assay Kit from Thermo Scientific (CA, USA). The proteins were fractionated using SDS polyacrylamide gel electrophoresis with a separation matrix comprising 10 and 15% polyacrylamide. The proteins were then transferred onto a polyvinylidene fluoride (PVDF) membrane. To prevent the non-specific binding of the primary antibodies, we blocked the PVDF membranes using a 5% skim milk solution in PBST for 1 h at room temperature. Following this, the membranes were incubated with the relevant primary antibodies overnight at 4 °C with gentle shaking. After primary antibody incubation, the membrane was washed with PBST. Subsequently, the membrane was developed by incubating with a secondary antibody for 1 h at room temperature. Following the secondary antibody incubation, the PVDF membranes were washed with PBST. The visualization of the membranes was carried out using chemiluminescence following the manufacturer's instructions provided by Invitrogen (CA, USA). Antibodies used were: CREB5 (ab168928; Abcam, Cambridge, UK), CD133 (ab278053; Abcam, Cambridge, UK), GFAP (840001; BioLegend, CA, USA), GAPDH (14C10; Cell Signaling, MA, USA), FLAG (F1804, Sigma Aldrich, MO, USA), and  $\beta$ -actin (A5316; Sigma Aldrich, MO, USA).

### Dataset analysis using public datasets

The mRNA expression levels of the CREB family were compared among various GSC cultures using the Gene Expression Omnibus (GSE4536) datasets. The gene expressions were normalized using the dChip invariant method, and the PM-MM difference model was used to calculate the expression values. Furthermore, the analysis of CREB5 gene expression profiles and correlation analysis with patient survival and other GSC related genes was conducted using the Rembrandt dataset obtained from the Gliovis website (<http://gliovis.bioinfo.cnio.es/>).

### Lentiviral infection for CREB5 knockdown

Lentiviral vectors were used to express non-targeting shRNA (shNT) and shRNA constructs targeting CREB5 (TRCN0000271247, TRCN0000013487;

Sigma Aldrich, MO, USA) to suppress CREB5 expression. To package the lentivirus, 293FT cells (Invitrogen, CA, USA) were transfected using the CalPhos Mammalian Transfection Kit (Takara Bio, Tokyo, Japan). We used pMD2.G and psPAX2 as packaging plasmids. The lentivirus was harvested 72 h after transfection and concentrated 100 fold with the Lenti-X concentrator (Takara Bio, Tokyo, Japan). Lentivirus infection was carried out following the manufacturer's protocol.

### Cell viability

The cell viability of GSCs after shRNA transduction was assessed using the alamarBlue® cell viability assay (Invitrogen, CA, USA). The shRNA transduced GSCs were seeded at a density of 3000 cells/well ( $n = 6$ ) in 96 well plates and incubated for 72 h. Then, 10  $\mu$ l of alamarBlue reagent was added to each well and incubated for an additional 6 h. After the incubation period, fluorescence was measured at a wavelength of 590 nm using a Synergy HTX Multi Mode Reader (VT, BioTek Instruments Inc., USA).

### In vitro limiting dilution assay

An in vitro limiting dilution assay was performed to assess the tumor sphere formation ability of shRNA transduced GSCs. The shRNA transduced GSCs were seeded in decreasing cell numbers (50, 25, 12, 6, 3, and 1 cell/well;  $n = 30$ ) in a 96 well plate. Cells were supplemented with 10  $\mu$ l growth media every after 3 days and maintained until 14 days. The plates were examined under a light microscope at the end of the incubation period for tumor sphere formation. Cell clusters measuring more than 20  $\mu$ m in diameter were considered to be positive wells. The frequency of tumor sphere formation ability of the GSCs was determined using the Extreme Limiting Dilution Analysis (ELDA) software, which can be accessed at <http://bioinf.wehi.edu.au/software/elda> [39]

### Annexin-V and propidium iodide staining

GSC11 and GSC23 were treated with shNT or shCREB5 for 72 h. After that, the cells were collected and washed with cold PBS. The cells were then incubated with Annexin-V and propidium iodide (Invitrogen, CA, USA) at room temperature for 15 min and analyzed using flow cytometry (Beckman Coulter, CA, USA).

### RNA-sequencing

GSCs were transduced with either shNT or shCREB5 and cultured in a 6 well plate for 2 days before harvesting at a density of  $5 \times 10^5$  cells. After washing with PBS, the cell pellets were resuspended in TRIzol Reagent (Invitrogen, CA, USA) and stored at  $-80^\circ\text{C}$ . RNA extraction, library preparation, and sequencing were outsourced to LAS Co., Ltd. (Gimpo, Republic of Korea).

### In vivo orthotopic implantation

For in vivo orthotopic implantation, shNT or shCREB5 treated GSCs were intracranially injected into the brains of BALB/c nude mice (female, 5 weeks old) at a concentration of  $5 \times 10^5$  cells using a stereotaxic instrument at coordinates of 2 mm right and 1.0 mm anterior of the bregma (randomization of  $n = 6$  mice per group). Mice that lost more than 30% of their body weight were sacrificed by established ethical protocols. The overall survival curves were generated using the Kaplan–Meier method. To perform tissue histological analysis, one mouse from both the control and experimental groups was sacrificed simultaneously one month after the GSC injection. All experiments involving mice were carried out in compliance with the applicable standards and regulations of the Republic of Korea government and the institution and were authorized by the Animal Care Committee of Chonnam National University (CNU/ACUC-YB-2021-99).

### Kyoto Encyclopedia of Genes and Genomes (KEGG) and Gene Ontology Biological Process (GO-BP) pathway analysis

To identify the genes that were downregulated by shCREB5, we performed KEGG pathway and GO-BP analysis using the DAVID website [40, 41].

### Luciferase reporter assay

To amplify the OLIG2 promoter fragment, Human Genomic DNA (Promega, WI, USA) was used as the source material. The OLIG2 promoter region was obtained by PCR amplification and then ligated into the pGL3-Basic vector (Promega, WI, USA) following the manufacturer's instructions. HEK293T cells were transfected in a 24 well plate at 70% confluence using Lipofectamine

2000 (Thermo Scientific, CA, USA). After 48 h, luciferase activity was measured using the dual luciferase reporter system (Promega, WI, USA) and normalized to the expression of *Renilla* luciferase. All experimental procedures were performed in triplicate.

### Chromatin immunoprecipitation (ChIP) assay

To crosslink chromatin associated proteins to DNA, approximately  $1 \times 10^7$  cells were treated with 37% formaldehyde for 10 min in a 100 mm culture dish. Then, glycine was added to quench the unreacted formaldehyde. The cells were collected in 1 ml of sodium dodecyl sulfate lysis buffer with 1  $\mu$ l of protease inhibitor cocktail added. The lysates were sonicated for 15 mins using 30 secs pulses at 30% output to fragment the DNA into pieces ranging from 200 to 1000 base pairs. After clearing the lysates by centrifugation at 13,000 rpm for 10 mins at  $4^\circ\text{C}$ , 200  $\mu$ l of the lysates were mixed with 1800  $\mu$ l of dilution buffer, and 60  $\mu$ l of protein A/G agarose (Thermo Scientific, CA, USA) was added. The mixture was then incubated at  $4^\circ\text{C}$  for 1 h to preclear the chromatin. The precleared lysates were then incubated overnight at  $4^\circ\text{C}$  with rotation with Flag antibody or normal mouse immunoglobulin G as a negative control. Immunoprecipitation of the DNA-protein complexes was performed using 60  $\mu$ l of protein A/G agarose (Thermo Scientific, CA, USA) for 1 h at  $4^\circ\text{C}$ , followed by isolation of the DNA. The human OLIG2 promoter was amplified by q-PCR, and all ChIP assays were performed three times. The following primer sequences: P1: F, GCATCCGAGATCTGCAGAAACAA and R, TACAGGCAGCCACCTGTCTC; P2: F, TGGGTGAATGCATCCGTACCT and R, TTACCGATTGCAGGCTGGCT; P3: F, GCCAAATGCCACGTGTTGA and R, CAGGATCCGGGGCTGGG; P4: F, TGAC-CACGTTCCCTTCTCCT and R, CCTCCTGCGCACAAACCAATG; P5: F, CCCAA-GAATCTCCCGGCCAC and R, AAGCTGATGTCATCCGGGCT.

### Statistical analysis

For statistical analysis, we used Microsoft Excel and GraphPad Prism Ver.9.0 software. To assess the significance between the two groups, we performed Student's *t* test in GraphPad Prism. To evaluate the statistical significance among multiple groups, we conducted a one-way analysis of variance (ANOVA), followed by Tukey's multiple comparison test. We considered the *p*-value less than 0.05 as statistically significant.

### DATA AVAILABILITY

The datasets generated during and/or analyzed during the current study are available in the NCBI SRA [PRJNA954560](https://www.ncbi.nlm.nih.gov/sra/PRJNA954560) repository.

### REFERENCES

- Lapointe S, Perry A, Butowski NA. Primary brain tumours in adults. *Lancet*. 2018;392:432–46.
- Chinot OL, Wick W, Mason W, Henriksson R, Saran F, Nishikawa R, et al. Bevacizumab plus Radiotherapy–Temozolomide for Newly Diagnosed Glioblastoma. *N Engl J Med*. 2014;370:709–22.
- Jordan CT, Guzman ML, Noble M. Cancer stem cells. *N Engl J Med*. 2006;355:1253–61.
- Prager BC, Bhargava S, Mahadev V, Hubert CG, Rich JN. Glioblastoma Stem Cells: Driving Resilience through Chaos. *Trends Cancer*. 2020;6:223–35.
- Nomura N, Zu YL, Maekawa T, Tabata S, Akiyama T, Ishii S. Isolation and characterization of a novel member of the gene family encoding the cAMP response element-binding protein CRE-BP1. *J Biol Chem*. 1993;268:4259–66.
- Impey S, McCorkle SR, Cha-Molstad H, Dwyer JM, Yochum GS, Boss JM, et al. Defining the CREB regulon: A genome-wide analysis of transcription factor regulatory regions. *Cell*. 2004;119:1041–54.
- Hai T, Hartman MG. The molecular biology and nomenclature of the activating transcription factor/cAMP responsive element binding family of transcription factors: activating transcription factor proteins and homeostasis. *Gene*. 2001;273:1–11.
- He S, Deng Y, Liao Y, Li X, Liu J, Yao S. CREB5 promotes tumor cell invasion and correlates with poor prognosis in epithelial ovarian cancer. *Oncol Lett*. 2017;14:8156–61.
- Wu J, Wang S-T, Zhang Z-J, Zhou Q, Peng B-G. Original Article CREB5 promotes cell proliferation and correlates with poor prognosis in hepatocellular carcinoma. *Int J Clin Exp Pathol*. 2018;11:4908–16.
- Wang S, Qiu J, Liu L, Su C, Qi L, Huang C, et al. CREB5 promotes invasiveness and metastasis in colorectal cancer by directly activating MET. *J Exp Clin Cancer Res*. 2020;39:168.
- Hwang JH, Seo JH, Beshiri ML, Wankowicz S, Liu D, Cheung A, et al. CREB5 Promotes Resistance to Androgen-Receptor Antagonists and Androgen Deprivation in Prostate Cancer. *Cell Rep*. 2019;29:2355–70.e6.

12. Lee J, Kotliarova S, Kotliarov Y, Li A, Su Q, Donin NM, et al. Tumor stem cells derived from glioblastomas cultured in bFGF and EGF more closely mirror the phenotype and genotype of primary tumors than do serum-cultured cell lines. *Cancer Cell*. 2006;9:391–403.
13. Verhaak RGW, Hoadley KA, Purdom E, Wang V, Qi Y, Wilkerson MD, et al. Integrated Genomic Analysis Identifies Clinically Relevant Subtypes of Glioblastoma Characterized by Abnormalities in PDGFRA, IDH1, EGFR, and NF1. *Cancer Cell*. 2010;17:98–110.
14. Suvà ML, Rheinbay E, Gillespie SM, Patel AP, Wakimoto H, Rabkin SD, et al. Reconstructing and reprogramming the tumor-propagating potential of glioblastoma stem-like cells. *Cell*. 2014;157:580–94.
15. Lu QR, Park JK, Noll E, Chan JA, Alberta J, Yuk D, et al. Oligodendrocyte lineage genes (OLIG) as molecular markers for human glial brain tumors. *Proc Natl Acad Sci USA*. 2001;98:10851–6.
16. Ligon KL, Alberta JA, Kho AT, Weiss J, Kwaan MR, Nutt CL, et al. The Oligodendroglial Lineage Marker OLIG2 Is Universally Expressed in Diffuse Gliomas. *J Neuropathol Exp Neurol*. 2004;63:499–509.
17. Singh SK, Fiorelli R, Kupp R, Rajan S, Szeto E, Lo Cascio C, et al. Post-translational Modifications of OLIG2 Regulate Glioma Invasion through the TGF- $\beta$  Pathway. *Cell Rep*. 2016;16:950–66.
18. Lu QR, Sun T, Zhu Z, Ma N, Garcia M, Stiles CD, et al. Common Developmental Requirement for Olig Function Indicates a Motor Neuron/Oligodendrocyte Connection. *Cell*. 2002;109:75–86.
19. Zhou Q, Anderson DJ. The bHLH Transcription Factors OLIG2 and OLIG1 Couple Neuronal and Glial Subtype Specification. *Cell*. 2002;109:61–73.
20. Takebayashi H, Nabeshima Y, Yoshida S, Chisaka O, Ikenaka K, Nabeshima Y-I. The Basic Helix-Loop-Helix Factor Olig2 Is Essential for the Development of Motoneuron and Oligodendrocyte Lineages. *Curr Biol*. 2002;12:1157–63.
21. Lu F, Chen Y, Zhao C, Wang H, He D, Xu L, et al. Olig2-Dependent Reciprocal Shift in PDGF and EGF Receptor Signaling Regulates Tumor Phenotype and Mitotic Growth in Malignant Glioma. *Cancer Cell*. 2016;29:669–83.
22. Shtayer L, Shtayer L, Tien AC, Szeto E, Sanai N, Rowitch DH, et al. Lineage-Restricted OLIG2-RTK Signaling Governs the Molecular Subtype of Glioma Stem-like Cells. *Cell Rep*. 2016;16:2838–45.
23. Ligon KL, Huillard E, Mehta S, Kesari S, Liu H, Alberta JA, et al. Olig2-Regulated Lineage-Restricted Pathway Controls Replication Competence in Neural Stem Cells and Malignant Glioma. *Neuron*. 2007;53:503–17.
24. Chong CR, Jänne PA. The quest to overcome resistance to EGFR-targeted therapies in cancer. *Nat Med*. 2013;19:1389–400.
25. Brennan C, Momota H, Hambardzumyan D, Ozawa T, Tandon A, Pedraza A, et al. Glioblastoma subclasses can be defined by activity among signal transduction pathways and associated genomic alterations. *PLoS One*. 2009;4:e7752.
26. Stommel JM, Kimmelman AC, Ying H, Nabioullin R, Ponugoti AH, Wiedemeyer R, et al. Coactivation of Receptor Tyrosine Kinases Affects the Response of Tumor Cells to Targeted Therapies. *Science*. 2007;318:287–90.
27. Vivanco I, Sawyers CL. The phosphatidylinositol 3-kinase-AKT pathway in humancancer. *Nat Rev Cancer*. 2002;2:489–501.
28. Degirmenci U, Wang M, Hu J. Targeting Aberrant RAS/RAF/MEK/ERK Signaling for Cancer Therapy. *Cells*. 2020;9:198.
29. Caglar HO, Duzgun Z. Identification of upregulated genes in glioblastoma and glioblastoma cancer stem cells using bioinformatics analysis. *Gene*. 2023;848:146895.
30. Messina S, Frati L, Leonetti C, Zuchegna C, Di Zazzo E, Calogero A, et al. Dual-specificity phosphatase DUSP6 has tumor-promoting properties in human glioblastomas. *Oncogene*. 2011;30:3813–20.
31. Liu Z, Ge R, Zhou J, Yang X, Cheng KK, Tao J, et al. Nuclear factor IX promotes glioblastoma development through transcriptional activation of Ezrin. *Oncogenesis*. 2020;9:39.
32. Ge R, Wang C, Liu J, Jiang H, Jiang X, Liu Z. A Novel Tumor-Promoting Role for Nuclear Factor IX in Glioblastoma Is Mediated through Transcriptional Activation of GINS1. *Mol Cancer Res*. 2023;21:189–98.
33. Nowicki MO, Hayes JL, Chiocca EA, Lawler SE. Proteomic analysis implicates Vimentin in Glioblastoma cell migration. *Cancers*. 2019;11:466.
34. Zottel A, Novak M, Šamec N, Majc B, Colja S, Katrašnik M, et al. Anti-Vimentin Nanobody Decreases Glioblastoma Cell Invasion In Vitro and In Vivo. *Cancers*. 2023;15:573.
35. Turtoi A, Musmeci D, Naccarato AG, Scatena C, Orteni V, Kiss R, et al. Sparc-like protein 1 is a new marker of human glioma progression. *J Proteome Res*. 2012;11:5011–21.
36. Gagliardi F, Narayanan A, Gallotti AL, Pieri V, Mazzoleni S, Cominelli M, et al. Enhanced SPARCL1 expression in cancer stem cells improves preclinical modeling of glioblastoma by promoting both tumor infiltration and angiogenesis. *Neurobiol Dis*. 2020;134:104705.
37. He W, Wang Y, Yang R, Ma H, Qin X, Yan M, et al. Molecular Mechanism of Naringenin Against High-Glucose-Induced Vascular Smooth Muscle Cells Proliferation and Migration Based on Network Pharmacology and Transcriptomic Analyses. *Front Pharmacol*. 2022;13:862709.
38. Bhat KPL, Balasubramanian V, Vaillant B, Ezhilarasan R, Hummelink K, Hollingsworth F, et al. Mesenchymal Differentiation Mediated by NF- $\kappa$ B Promotes Radiation Resistance in Glioblastoma. *Cancer Cell*. 2013;24:331–46.
39. Hu Y, Smyth GK. ELDA: Extreme limiting dilution analysis for comparing depleted and enriched populations in stem cell and other assays. *J Immunol Methods*. 2009;347:70–8.
40. Sherman BT, Hao M, Qiu J, Jiao X, Baseler MW, Lane HC, et al. DAVID: a web server for functional enrichment analysis and functional annotation of gene lists (2021 update). *Nucleic Acids Res*. 2022;50:216–21.
41. Huang DW, Sherman BT, Lempicki RA. Systematic and integrative analysis of large gene lists using DAVID Bioinformatics Resources. *Nature Protoc*. 2009;4:44–57.

## ACKNOWLEDGEMENTS

This research received comprehensive support from several funding sources. It was primarily supported by the Basic Science Research Program through the National Research Foundation of Korea (NRF), with funding from the Ministry of Education, Science and Technology under grant number 2022R111A3070961. Additionally, it benefited from the support of the National Research Foundation of Korea (NRF) grant, funded by the Ministry of Science and ICT (MSIT) under grant number 2022R1A5A8033794. The National Institute of Fisheries Science in Korea also contributed to this study through grant R2023054. Further support was provided by the BK21 FOUR (Fostering Outstanding Universities for Research) program, which is funded by the Ministry of Education and the National Research Foundation of Korea. Moreover, the World Institute of Kimchi extended its support through grant KE2301-2, funded by the Ministry of Science and ICT, Republic of Korea.

## AUTHOR CONTRIBUTIONS

The study was conceptualized by HJK, HMJ and SHK. The *in vitro* and *in vivo* experiments were conducted and analyzed by HJK and HMJ. DCB carried out some of the *in vitro* experiments. MP, SJL, and JBS conducted and analyzed the *in-silico* analyses. The instruments for the *in vivo* experiments were provided by SL, YJO, and SIP. JH and JY provided some of the reagents used in the research. The manuscript was written by HJK, SSS, and SHK, with contributions from all authors. The study was supervised by SSS and SHK.

## COMPETING INTERESTS

The authors declare no competing interests.

## ADDITIONAL INFORMATION

**Supplementary information** The online version contains supplementary material available at <https://doi.org/10.1038/s41420-024-01873-z>.

**Correspondence** and requests for materials should be addressed to Sung-Suk Suh or Sung-Hak Kim.

**Reprints and permission information** is available at <http://www.nature.com/reprints>

**Publisher's note** Springer Nature remains neutral with regard to jurisdictional claims in published maps and institutional affiliations.



**Open Access** This article is licensed under a Creative Commons Attribution 4.0 International License, which permits use, sharing, adaptation, distribution and reproduction in any medium or format, as long as you give appropriate credit to the original author(s) and the source, provide a link to the Creative Commons licence, and indicate if changes were made. The images or other third party material in this article are included in the article's Creative Commons licence, unless indicated otherwise in a credit line to the material. If material is not included in the article's Creative Commons licence and your intended use is not permitted by statutory regulation or exceeds the permitted use, you will need to obtain permission directly from the copyright holder. To view a copy of this licence, visit <http://creativecommons.org/licenses/by/4.0/>.